Determination of Kinetic Rate Constants for the Binding of Inhibitors to HIV-1 Protease and for the Association and Dissociation of Active Homodimer

Christopher A. Pargellis,*,‡ Maurice M. Morelock,‡ Edward T. Graham,§ Peter Kinkade,‡ Susan Pav,‡ Klaus Lubbe,∥ Daniel Lamarre,⊥ and Paul C. Anderson∞

Departments of Biochemistry, Information Systems, and Pharmaceutics, Boehringer Ingelheim Pharmaceuticals, Inc., 900 Ridgebury Road, P.O. Box 368, Ridgefield, Connecticut 06877, and Departments of Biochemistry and Medicinal Chemistry, Bio-Mega/Boehringer Ingelheim Research, Inc., 2100 rue Cunard, Laval, Quebec, Canada H7S 2G5

Received April 11, 1994; Revised Manuscript Received July 12, 1994®

ABSTRACT: Association and dissociation rate constants for a competitive inhibitor of HIV-1 protease were determined by a novel method employing a pair of integrated rate equations. This method, termed the paired progress curve method, is both rapid and reproducible. Progress curves, taken at a single concentration of inhibitor, are analyzed simultaneously to determine association and dissociation rate constants, the concentration of active sites, and the catalytic rate constant. The method is applied to BILA 398, a compound for which the cocrystal structure with HIV-2 protease has been reported recently [Tong, L., et al. (1993) *Proc. Natl. Acad. Sci. U.S.A. 90*, 8387–8391]. This compound exhibited an association constant of 1.6×10^7 M^{-1} s^{-1} and a dissociation constant of 1.0×10^{-4} s^{-1} corresponding to a binding affinity constant of 6.4×10^{-12} M. During the course of the analysis, nonlinearity was observed in control reactions containing enzyme and substrate only. This was subsequently shown to be due to a reversible inactivation process resulting from enzyme dilution. Integrated rate equations were developed on the basis of the dissociation of active dimeric enzyme during dilution and a reassociation of dilute monomers following the addition of substrate. The equations were modeled to the data, yielding a dissociation constant of 1.9×10^{-3} s^{-1} and an association constant of 9.2×10^5 M^{-1} s^{-1} for the monomer–dimer interconversion process. This corresponds to an equilibrium constant of 4×10^{-9} M for the dimerization of HIV-1 protease.

Human immunodeficiency virus (HIV[1]) is the etiological agent of AIDS. The clinically relevant strain, HIV-1, has been the focus of intense research investigations over the last several years (Debouck & Metcalf, 1990). HIV protease, one of three *pol* gene products encoded for by the virus, functions in the maturation of many viral proteins. These viral proteins are present initially as long polyproteins that require cleavage at specific sites for the generation of smaller, active proteins. The inhibition of HIV protease activity in cell culture has been demonstrated to inhibit viral infectivity (Kaplan et al., 1993), and several inhibitors of HIV protease are currently undergoing clinical trials for the treatment of AIDS.

HIV protease will also cleave small peptides based on the known amino acid sequences of the polyprotein cleavage sites. This characteristic has been exploited in the development of many different assay systems. Substrates can be either chromogenic or fluorogenic, which allows for the continual monitoring of substrate conversion to product (Matayoshi et al., 1990). Peptidomimetics of the transition states of these peptide substrates, such as the reduced amide bond inhibitor reported here, are often found to be very potent inhibitors of HIV protease (Debouck & Metcalf, 1990).

HIV protease is an obligate homodimeric enzyme that is able to dissociate and reassociate freely under *in vitro* conditions (Cheng et al., 1990; Zhang et al., 1991). A tethered dimeric enzyme can be engineered that is no longer able to dissociate into inactive monomers. The insertion of these tethered dimers into the viral genome leads to the inhibition of virion particle assembly, suggesting that the ability of HIV protease to dimerize and monomerize *in vivo* is essential for accurate viral replication (Kräusslich, 1991). An additional class of inhibitors, which takes advantage of the homodimeric nature of HIV protease by mimicking the symmetrical interface region between monomers, is also under active investigation (Babé et al., 1992). A technique (presented herein) for the determination of the association and dissociation rate constants (k_{assoc} and k_{dis}, respectively) would be of great value in further evaluating these types of inhibitors.

The most widely cited thermodynamic parameter used in the analysis of enzyme inhibitors is the inhibition constant, K_i. Lists of K_i values typically arise from structure–activity studies in which an inhibitor is optimized for potency. Much less frequently, the association and dissociation rate constants (k_{on} and k_{off}, respectively) are reported. These kinetic constants are more difficult to determine as they require time-based experimental techniques for data acquisition and the implementation of complex mathematical equations for data analysis. The dissociation rate constant is the most critical value for the selection of a drug candidate, as lower k_{off} values correspond to longer half-lives for the inactive enzyme–inhibitor (EI) complex. Since K_i is the ratio of k_{off} to k_{on}, many different pairs of k_{off}/k_{on} can give rise to the same K_i.

* Author to whom correspondence should be addressed.

‡ Department of Biochemistry, Boehringer Ingelheim Pharmaceuticals, Inc.

§ Department of Information Systems, Boehringer Ingelheim Pharmaceuticals, Inc.

∥ Department of Pharmaceutics, Boehringer Ingelheim Pharmaceuticals, Inc.

⊥ Department of Biochemistry, Bio-Mega/Boehringer Ingelheim Research, Inc.

∞ Department of Medicinal Chemistry, Bio-Mega/Boehringer Ingelheim Research, Inc.

® Abstract published in *Advance ACS Abstracts*, October 1, 1994.

[1] Abbreviations: HIV, human immunodeficiency virus; AIDS, acquired immune deficiency syndrome; RNA, ribonucleic acid; IPTG, isopropyl β-D-thioglucopyranoside; PMSF, phenylmethanesulfonyl floride; EDTA, ethylenediaminetetraacetate; HPLC, high-pressure liquid chromatography; BSA, bovine serum albumin.

0006-2960/94/0433-12527$04.50/0

Hence, an analysis based on K_i values alone would overlook those inhibitors exhibiting the very desirable properties of being both slow binding and slow dissociating (Frieden et al., 1980).

The time course for the inhibition process (i.e., the progress curve of the reaction) must be obtained for the determination of k_{off} and k_{on}. These experiments can arise from either the onset of inhibition or the dissociation of preformed EI complexes. The computational analysis consists of fitting these nonlinear data to rate equations describing the conversion of substrate to product. Early attempts to fit fully integrated rate equations describing either the onset of inhibition by a tight-binding inhibitor or the dissociation of an EI complex were unsuccessful (Cha, 1980). Consequently, numerical approximation methods and the use of parametric equations have been employed to circumvent tedious derivations of analytical solutions and to simplify the regression process (Zimmerle & Frieden, 1989; Sculley & Morrison, 1986; Morrison & Stone, 1985). These methods allow the evaluation of complex phenomena involving multiple intermediates.

Routine analytical methods in use today break the computational analysis into multiple steps, overcoming the mathematical difficulties encountered earlier. Typically, nonlinear regression techniques are first applied to a family of progress curves for the onset of inhibition to obtain steady state velocities (v_s). Then, in a second step, pairs of v_s and total inhibitor concentrations ($[I]_T$) are fitted with an equation describing steady state conditions to yield estimates for K_i and the total enzyme concentration ($[E]_T$). In the final step, the same progress curves are fitted (with fixed values of K_i and/or $[E]_T$) to integrated rate equations, yielding estimates for k_{off} and k_{on} (Williams et al., 1979).

The multistep methods of analysis have several significant defects. First, it frequently is not possible to achieve convergence without bias (i.e., collinearity) when data from only an association or a dissociation experiment are being analyzed. This is because an association data set is primarily dependent on k_{on}, while a dissociation data set is primarily dependent on k_{off}, resulting in a bias for the less weighted rate constant. Second, the statistical error of the parameter estimates resulting from the final step requires the use of complex propagation of error techniques (Bevington, 1969) in order to carry forward statistical error from earlier steps. These techniques are difficult to perform, are of questionable value when applied to nonlinear systems, and hence, are rarely determined. Finally, setting any parameter to a fixed value in a multistep analysis without using propogation of error techniques negates any error information carried forward and may actually result in nonconvergence due to data variability. An analysis in which all kinetic parameters are estimated simultaneously in a single regression step would not be expected to possess these defects.

In this report, a single-step nonlinear regression analysis is applied to both association and dissociation data simultaneously for the determination of kinetic rate constants. This method will determine $[E]_T$, k_{on}, k_{off}, and the catalytic rate constant (k_{cat}) with acceptable statistics, in contrast to current multistep methods. No additional information about the system is required, except for the Michaelis–Menten constant (K_m), thus precluding the need for the independent determination of $[E]_T$ and K_i. The experimental method is very rapid as progress curves are generated at a single [I]. The technique is successfully applied to the HIV-1 protease system in the determination of (1) the inactivation rate of a tight-binding inhibitor and (2) the interconversion rates of an inactive monomer with active homodimer.

EXPERIMENTAL PROCEDURES

Inhibitors. Details of the active site binding inhibitor, BILA 398, can be found in previously published work (Tong et al., 1993).

Expression and Preparation of Enzyme. The HIV-1 protease gene was amplified by the polymerase chain reaction from pBH10 (Hahn et al., 1984) and subcloned into the T7 expression vector pET11d using the *Xba*I and *Bam*HI restriction sites for expression in *Escherichia coli* BL21(DE3)-plysS cells (Studier et al., 1990). The DNA fragment encodes for the mature protease by providing in-frame translation start and stop codons. A 10 L fermentation was conducted as described (Studier & Moffat, 1986). Oxygen was kept above 10% air saturation, pH was maintained at 6.5, and glucose was above 1 gm/L. Induction of expression began by the addition of IPTG at an optical density (560 nm) of 15–20. The culture was harvested 2 h after induction. Final centrifugation typically yielded 400–500 g of wet cell paste, which was stored at −80 °C until lysis and purification. Cell paste (100–200 g) was thawed by the addition of an equal volume of cold 50 mM Tris, 25 mM NaCl, 100 mM KCl, 0.5% (v/v) Triton X-100, 5 mM EDTA, and 1 mM DTT (pH 8.0) at 4 °C. An equal volume of 2 mg/mL lysozyme in the same buffer was added to the thawed volume, along with PMSF to 1 mM. After the mixture rested on ice for about 20 min, $MgCl_2$ was added to 10 mM, followed by the addition of ribonuclease I to 20 μg/mL. Lysis was performed in a Parr cell disruption bomb. The sample was equilibrated in the chamber at 4 °C for 30 min at 1500 psi with stirring. Lysate was gradually released through the outlet valve while a constant pressure of 1400–1500 psi was maintained within the chamber. EDTA was added to 15 mM and PMSF to 1 mM prior to centrifugation at 12 000 rpm (14700*g*) for 1 h at 5–15 °C. Pellets were combined and washed by sonication in wash buffer (2 M urea, 50 mM sodium acetate (pH 5.5), 1 mM disodium EDTA, and 2.5 mM dithiothreitol) and recentrifuged. Pellets from the second centrifugation were combined, and inactive HIV-1 protease was extracted by sonication in solubilization buffer (8 M urea, 50 mM sodium acetate (pH 5.5), 1 mM disodium EDTA, and 2.5 mM dithiothreitol). Aliquots of the urea extract (38 mL) were applied to a 5 × 55 cm size exclusion chromatographic column packed with Superdex 200PG (Pharmacia Biotech, Inc., Piscataway, NJ) equilibrated in 8 M urea, 100 mM sodium acetate (pH 5.5), and 1 mM dithiothreitol. Aliquots of fractions were diluted with 9 vol of refolding buffer [50 mM sodium acetate (pH 5.5), 1 mM disodium EDTA, 0.2% (w/v) NP-40, 10% (w/v) glycerol, 5% (w/v) ethylene glycol, 0.01% (w/v) sodium azide, and 1 mM dithiothreitol] and assayed for HIV-1 protease activity. Hydrolysis of the substrate fluorescein–VSFNF*PQITL was monitored by HPLC using a Perkin-Elmer 3 × 3 CR8, 3 μm column. The column was eluted at 3 mL/min in 36% (v/v) acetonitrile and 0.1% trifluoroacetic acid. Peptide hydrolysis was monitored using a Hewlett-Packard 1046A fluorescence detector set at an excitation wavelength of 425 nm and an emission wavelength of 518 nm. Fractions containing the majority of biological activity were pooled from three separate size exclusion chromatographic runs. An aliquot of the size exclusion chromatographic pool (38 mL) was applied to a 2.2 × 25 cm 214TP 1520 Vydac C4 column (The Separations Group, Hesparia, CA) and eluted with a linear gradient of acetonitrile/water/trifluoroacetic acid 31.5:68.5:0.1 to acetonitrile/water/trifluoroacetic acid 58.5:41.5:0.1. The reversed phase HPLC fractions (4.5 mL) were concentrated to dryness under reduced pressure and then reconstituted in 1 mL of solubilization buffer. Fractions containing the majority

of HIV-1 protease activity were pooled. The reversed phase purified pool was diluted with 9 vol of refolding buffer and stored in 1 mL aliquots at −80 °C.

Enzyme Activity Assay. Enzyme activity was determined by monitoring the fluorescence change associated with the cleavage of the fluorogenic substrate 2-aminobenzoyl-Thr-Ile-Nle-Phe(*p*-NO_2)-Gln-Arg-NH_2 (Bachem, Torrance, CA). Reactions were run at 23 °C in a final volume of 2.0 mL containing 100 mM sodium acetate, 4 mM EDTA, 0.5 M sodium chloride, 0.025% sodium azide and 1 mg/mL fatty acid free BSA at a pH of 5.5. Substrate was added to a final concentration of 1.0×10^{-5} M from a stock solution in DMSO. The final concentration of DMSO was brought to 1.0%. In a separate experiment, the substrate binding affinity or K_m was determined to be 4.11×10^{-6} M under these conditions (low salt) and 1.33×10^{-6} M at 1.5 M sodium chloride (high salt).

(a) Monomer–Dimer Exchange. The association of monomeric HIV protease was obtained by preincubating dilute enzyme for 60 min at 23 °C, in order to achieve a monomer/dimer equilibrium, prior to the addition of substrate. The dissociation of dimeric enzyme was determined by preincubating cuvettes containing substrate for 5 min at 23 °C prior to the addition of a high concentration of enzyme stock. The final active site concentration of HIV protease was about 1×10^{-10} M in both experiments. In both cases, substrate conversion to product was not allowed to exceed 20%.

(b) Inhibitor Binding. The onset of inhibition was obtained by preincubating substrate and inhibitor in buffer containing 1.5 M NaCl (high salt) for 5 min at 23 °C prior to the addition of enzyme. The dissociation of EI was obtained by preincubating enzyme and inhibitor at 23 °C for 60 min prior to the addition of substrate. The final active site concentration of HIV protease was about 1×10^{-9} M in both experiments, which is exactly 10-fold more concentrated than that used in the analysis of monomer–dimer interconversion described earlier. Substrate conversion to product was not allowed to exceed 25% in both cases. It was not possible to further decrease substrate conversion for the following reasons: decreasing $[E]_T$ results in increased curvature due to dimer dissociation, and shortening the reaction time course led to insufficient EI dissociation. However, control experiments run in the absence of inhibitor exhibited negligible downward curvature, indicating that reaction velocity is minimally affected by either substrate depletion or byproduct inhibition.

(c) K_i Determination. K_i was also determined by an independent and established method (Morrison & Stone, 1985; Greco & Hakala, 1979). Nonlinear association rate data were obtained at multiple $[I]_T$. The steady state velocity was estimated by fitting data to an integrated rate equation describing competitive binding. Pairs of v_s and $[I]_T$ values were fitted to the quadratic equation (eq 6) describing tight-binding inhibition. Further experiments, conducted at varying [S] (data not shown), established that $K_{i(app)}$ varied linearly with [S], implying a competitive mechanism of inhibition for this series of inhibitors (see Theory).

Fluorescence Detection of Product. The time course of the reaction was monitored using an SLM Aminco Bowman Series 2 Model SQ-340 fluorescence detector equipped with a high-speed 2-place magnetic stirrer. The excitation maximum of the product, 2-aminobenzoyl-Thr-Ile-Nle, was determined to be 330 nm with an emission maximum at 417 nm using a bandpass of 4.0 nm. The high-voltage setting of the photomultiplier tube was set at approximately 30% of saturation with substrate alone. Data for the dissociation and reassociation of HIV protease were collected as the ratio of emission to an internal electrical diode standard for 4000 s at an acquisition interval of 4.0 s. Data for the association and dissociation of enzyme and inhibitor were collected at an acquisition rate of 1.0 s for 400 s. In both cases, data acquisition began within 5 s after the initiation of the reaction.

Scheme 1

$$E + S \underset{}{\overset{K_m}{\rightleftharpoons}} ES \xrightarrow{k_{cat}} E + P$$

$$+$$

$$I \underset{k_{off}}{\overset{k_{on}}{\rightleftharpoons}} EI$$

Nonlinear Regression Analysis. Six data files (three paired progress curves) containing product measurements were normalized and combined. It was determined that a single set of paired progress curves was insufficient to ensure successful statistical analysis (consistent convergence). Data analysis was performed by applying ordinary nonlinear least-squares regression techniques to the selected model using the Marquardt–Levenberg minimization method. The parameters estimated were $[E]_T$, k_{cat}, k_{on}, and k_{off}. Convergence of the model occurs quickly with good initial estimates. Analysis can, however, become lengthy when initial estimates are determined from large arrays for those parameters that are least well-known. Fitting for k_{cat} provides an internal diagnostic as to the goodness of fit, although this constant is known with some certainty. Occasionally, the regression results in biased or unreasonable parameter estimates. This is typically caused by insufficient information in the dissociation progress curve, i.e., little or no curvature. In these cases it was necessary to fix one of the parameters, usually k_{cat}, for a solution. All of the data were analyzed using the SAS statistical software system (version 6.07, SAS Institute Incorporated, Cary, NC) on an HP Apollo 735 workstation (Hewlett-Packard Company, Palo Alto, CA).

THEORY

I. Competitive Inhibition. Substrate analogs and transition state inhibitors of HIV-1 protease typically are reversible tight-binding inhibitors (Debouck & Metcalf, 1990). Structural information indicates that BILA 398 occupies the substrate binding site of HIV-2 protease (Tong et al., 1993), and work with related inhibitors in our laboratory has established a competitive binding mode of inhibition (see Experimental Procedures). Examination of association rate data at various values of $[I]_T$ reveals no variation in initial velocity, indicating that a single-step formation of EI (Scheme 1) will adequately describe the data (Williams, et al., 1979).

Experimentally, association reactions are initiated by the addition of enzyme to a mixture of substrate and inhibitor; conversely, dissociation reactions are initiated by the addition of substrate to preincubated solutions containing preformed EI complexes. Downward curvature in the association data set (Figure 1) is due to the slow rate of EI complex formation. The slow association rate results from low concentrations of both $[E]_T$ and $[I]_T$, since k_{on} has been set to near the diffusion control limit in this particular case (see Figure 1 legend). Conversely, upward curvature in the dissociation data set is due to the slow rate of EI complex dissociation. These two reactions, taken together and at a single $[I]_T$, constitute a paired progress curve.

The derivation of an equation for the rate of change of the Michaelis complex to give product (eq 1) has been published

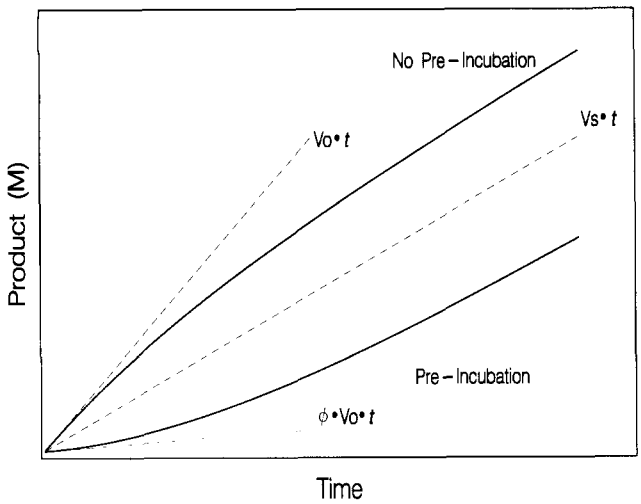

FIGURE 1: Theoretical paired progress curves for competitive inhibition. Association kinetics (downward curve) and dissociation kinetics (upward curve) are shown for the inhibition of HIV protease by a tight-binding inhibitor. The values for velocity at zero time are shown (straight lines). The following values for constants were used: $[E]_T = 2 \times 10^{-9}$ M, $[I]_T = 2 \times 10^{-9}$ M, $k_{on} = 1 \times 10^7$ M^{-1} s^{-1}, $k_{off} = 1 \times 10^{-4}$ s^{-1}, $k_{cat} = 8$, $K_s = 8 \times 10^{-7}$ M, and [S] = 8×10^{-5} M.

by a number of authors (Cha, 1980) (Williams & Morrison, 1979) and hence will not be given here.

$$[P]_t = [P]_0 + v_s t - \frac{(v_s - v_z)(1 - \gamma')}{\lambda\gamma'} \ln\left(\frac{1 - \gamma' e^{-\lambda t}}{1 - \gamma'}\right) \quad (1)$$

where $[P]_t$ is the product concentration at time t, $[P]_0$ is the product concentration at $t = 0$, v_z is the velocity at $t = 0$,

$$v_z = \phi v_0 \quad (2)$$

and v_0 is the uninhibited velocity

$$v_0 = \frac{k_{cat}[E]_T}{1 + K_m/[S]} \quad (3)$$

where $[E]_T$ is the total enzyme concentration, [S] is the substrate concentration, K_m is the Michaelis–Menten constant, and k_{cat} is the catalytic rate constant.

The symbol ϕ, shown in eq 2, is the fraction of active enzyme (free of inhibitor) at time zero. The value for ϕ will depend upon the presence or absence of an enzyme–inhibitor preincubation step. When the reaction is started by the addition of free enzyme to a mixture of substrate and inhibitor, then

$$\phi = 1 \quad (4)$$

as all of the enzyme is available for binding to substrate. When enzyme is preincubated with inhibitor ($[I]_T$ is the total inhibitor concentration), then ϕ will be given by

$$\phi = \frac{1}{2[E]_T}\left[[E]_T - K_i - [I]_T + \sqrt{(-[E]_T + K_i + [I]_T)^2 + 4[E]_T K_i}\right] \quad (5)$$

This preincubation occurs without substrate and proceeds to equilibrium. The paired progress curve method fits data to eq 1 simultaneously, with ϕ defined appropriately for both sets of data.

v_s is the steady state velocity given by

$$v_s = \frac{v_0}{2[E]_T}\left[[E]_T - K_i(app) - [I]_T + \sqrt{(-[E]_T + K_{i(app)} + [I]_T)^2 + 4[E]_T K_{i(app)}}\right] \quad (6)$$

The expression for $K_{i(app)}$ depends on the mechanism of inhibition and is given here for a competitive mode of inhibition.

$$K_{i(app)} = \frac{K_i}{1 + [S]/K_m} \quad (7)$$

The value for λ is given by

$$\lambda = \frac{q}{1 + [S]/K_m} \quad (8)$$

$$q = \{[k_{on}[I]_T - k_{on}[E]_T + k_{off}(q + [S]/K_m)]^2 + 4[k_{off}([S]/K_m)[E]_T][k_{on}(1 + K_m/[S])]\}^{1/2} \quad (9)$$

where k_{off} is the dissociation rate constant, k_{on} is the association rate constant, and finally the value for γ' is given by

$$\gamma' = \frac{[E]_T(2\phi - 1) + [I]_T + K_{i(app)} - q/k_{on}}{[E]_T(2\phi - 1) + [I]_T + K_{i(app)} + q/k_{on}} \quad (10)$$

The paired progress curve method uses both association and dissociation curves simultaneously at a single $[I]_T$. A solution for the experimentally selected value of $[I]_T$ needs to be found to give the best possible chance of a successful regression analysis. Computer simulations of paired progress curves (Figure 2) were generated at three different $[I]_T$ values using the model shown in Scheme 1 for a tight-binding inhibitor. If $[I]_T < [E]_T$, the paired progress curves are symmetrical but the amplitude ($|[P]_T - v_s t|$) is vanishingly small (Figure 2A); in contrast, if $[I]_T > [E]_T$, large asymmetry is observed (Figure 2B). Both small amplitude and large asymmetry are undesirable since (1) small amplitude indicates that the progress curves do not differ appreciably from the equilibrium condition, and (2) large asymmetry will cause the subsequent regression analysis to emphasize one curve over the other, resulting in bias. The paired progress curves are optimized for symmetry and amplitude only when $[I]_T \approx [E]_T$ (Figure 2C). Experimental constraints also prevent the use of extreme $[I]_T$: substrate turnover becomes significant when $[I]_T$ is small, and the detection of product becomes difficult when $[I]_T$ is large. Hence, a value for $[I]_T$ selected close to that of $[E]_T$ can be considered the optimal concentration of inhibitor ($[I]_{opt}$) for this particular set of experimental conditions (see legend to Figure 2).

These results can be generalized beyond this single set of experimental conditions to include other enzyme–inhibitor systems of interest. Since the initial inhibitor concentrations for the association and dissociation reactions result in extremes of inhibitor binding, i.e., [EI] = 0 for association and [EI] $\approx [E]_T$ for dissociation, it is desirable to determine an $[I]_{opt}$ values that will result in a balanced approach to equilibrium. Typically, the critical points for maximizing or minimizing a function with respect to a variable are determined by setting the respective derivative equal to zero and solving for the variable. The common critical point for the association and dissociation reactions can be determined by setting the derivatives of the function for [P] (eq 1) equal to each other, i.e., $(\partial[P]/\partial[I])_{assoc} = (\partial[P]/\partial[I])_{dis}$, and solving for $[I]_{opt}$. Due to the complexity of the $\partial[P]/\partial[I]$ equation, a numerical solution was obtained by graphical analysis. Figure 3 shows a plot of a pair of $\partial[P]/\partial[I]$ curves with the concentration of

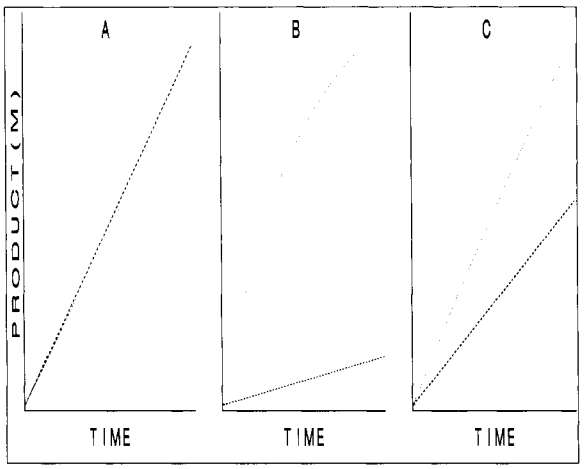

FIGURE 2: Effect of varying $[I]_T$ on theoretical paired progress curves. Progress curves were generated using three different values of $[I]_T$: (A) $[I]_T < [E]_T$ ($[I]_T = 2 \times 10^{-10}$ M); (B) $[I]_T > [E]_T$ ($[I]_T = 2 \times 10^{-8}$ M); and (C) $[I]_T = [E]_T$ ($[I]_T = 2 \times 10^{-9}$ M). All other constants are the same as given in the legend to Figure 1, and the dashed line shows $\nu_s t$.

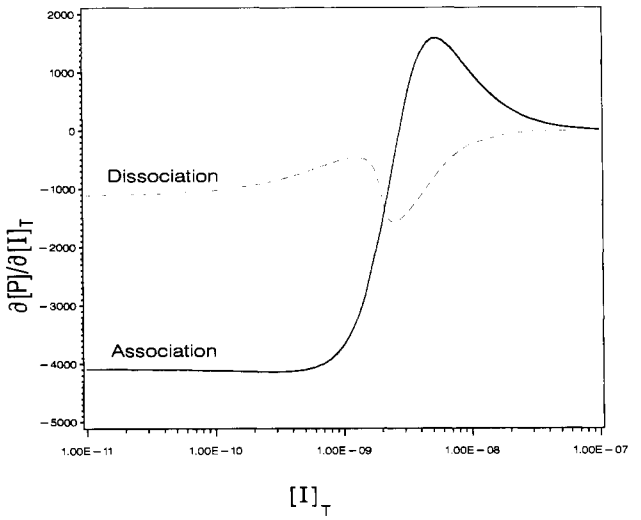

FIGURE 3: Variation of $\partial[P]/\partial[I]_T$. The derivative of changing [P] with changing $[I]_T$ is shown. The derivatives for the associative and dissociative phases are equal at a value approximately equal to $[E]_T$. All constants are the same as those given in the legend to Figure 1 except for $[I]_T$, which is varying as shown.

substrate set so that binding competition with inhibitor is equal (i.e., $[EI]/[E]_T = 0.5$ at equilibrium). Visual inspection as well as numerical analysis reveals that both derivatives are equal when $[I]_T \approx [E]_T$, thus determining $[I]_{opt}$. Note that this determination is the same as that made earlier (Figure 2) from the direct examination of paired progress curves. Derivatives of paired progress curves were generated for k_{on} ranging from 10^4 to 10^8 and for k_{off} ranging from 10^0 to 10^{-8}. $[I]_{opt}$ was observed to be constant for a given K_i at all k_{off}/k_{on} ratios (data not shown). A plot of the correlation between $[I]_{opt}$ and K_i is shown as a function of $[E]_T$ (Figure 4). The empirical fit to this data is given by

$$[I]_{opt} = [E]_T + K_i \quad (11)$$

Thus, $[I]_{opt} \approx [E]_T$ for tight-binding inhibitors ($K_i \leq [E]_T$), and $[I]_{opt} \approx K_i$ for classical inhibitors ($K_i > [E]_T$). It should be emphasized, however, that in this report, we have only examined tight-binding inhibitors with $[I]_{opt} \approx [E]_T$ and $K_i < [E]_T$. The apparent universal application of eq 11 has yet to be determined.

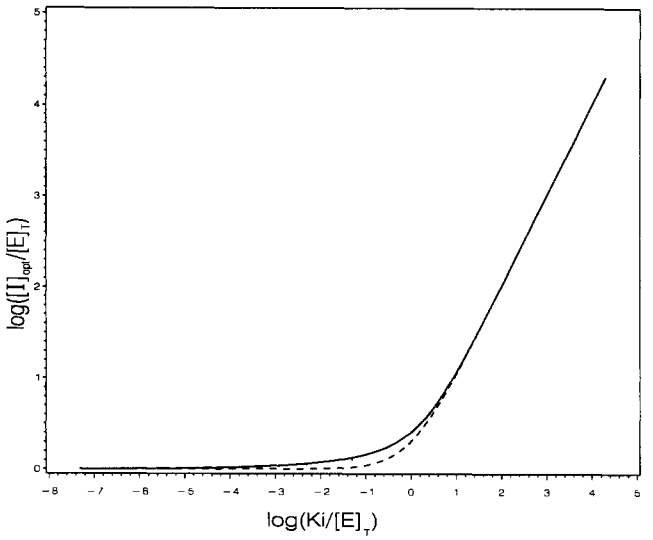

FIGURE 4: Numerical solution for $[I]_{opt}$ vs K_i as a function of $[E]_T$. Numerical solutions for the variation of $\partial[P]/\partial[I]$ as a function of $[I]_{opt}$ (solid line) and the corresponding fitted line for $[I]_{opt} = [E]_T + K_i$ (dashed line) are shown.

Scheme 2

$$M + M \underset{k_{dis}}{\overset{k_{assoc}}{\rightleftharpoons}} D + S \overset{K_m}{\rightleftharpoons} DS \xrightarrow{k_{cat}} D + P$$

Now that $[I]_{opt}$ has been determined, the optimal concentration of substrate ($[S]_{opt}$) can be calculated to give equal binding competition with inhibitor:

$$[S]_{opt} = \frac{1}{2}[E]_T K_m / K_i \quad (12)$$

$[S]_{opt}$, predicted by eq 12, represents the optimal conditions predicted by theory, which may not be achievable for experimental reasons. For example, if $K_i << [E]_T$ (as is true for BILA 398), then $[S]_{opt} \gg K_m$. Such high [S] may either exceed substrate solubility or result in inhibition due to high [S].

In summary, the experimental approach for the paired progress curve method is as follows: (1) determine K_m and K_i from steady state experiments; (2) calculate $[I]_{opt}$ and $[S]_{opt}$ from eqs 11 and 12, respectively; (3) generate paired progress curves (qualified by good symmetry, signal, and final velocity approaching ν_s); and (4) apply regression using the integrated rate equation to the combined paired progress curve data set.

II. Dimer Dissociation. The analysis of reversible enzyme inactivation by dimer dissociation is very similar to the analysis of reversible enzyme inhibition described earlier. Previous work (Grant et al., 1992) has demonstrated that a simple two-state model in which inactive monomers are converted to active dimers in a single step adequately describes the dissociation of HIV-1 protease. Other published work (Kuzmic et al., 1993) indicates that substrate binding stabilizes the dimer by competing with dimer dissociation. These elements are presented in Scheme 2.

The solution for the integrated rate equation describing this reversible inactivation process is identical to that given for competitive inhibition.

$$[P]_t = [P]_0 = \nu_s t - \frac{(\nu_s - \nu_z)(1-\gamma')}{\lambda\gamma'} \ln\left(\frac{1-\gamma' e^{-\lambda t}}{1-\gamma'}\right) \quad (1)$$

The definitions of the various terms, however, are different. ν_z is the velocity at $t = 0$

$$\nu_z = \phi\nu_0 \quad (13)$$

with ν_0 (the uninhibited velocity) now given by

$$\nu_0 = \frac{k_{cat}([M]_T/2)}{1 + K_m/[S]} \quad (14)$$

where $[M]_T$ is the total monomer concentration.

The symbol ϕ in eq 13 indicates the fraction of active dimer at time zero. The value for ϕ will depend upon whether an enzyme preincubation step has occurred. When the reaction is started by the addition of concentrated enzyme to substrate, then

$$\phi = 1 \quad (15)$$

since all of the enzyme is dimeric and available to bind substrate. When enzyme is preincubated at low concentration, then

$$\phi = \frac{1}{4[M]_T}\left[4[M]_T + K_d - \sqrt{8[M]_T K_d + K_d^2}\right] \quad (16)$$

where K_d is the dissociation constant for monomer–dimer exchange given by $K_d = 2k_{dis}/k_{assoc}$. The data are fit to eq 1 with ϕ defined appropriately.

The steady state velocity (ν_s) is given by

$$\nu_s = \nu_0 + \frac{K_d}{4[M]_T}\left(\frac{\nu_0}{1 + ([S]/K_m)}\right) - \frac{\nu_0}{4}\sqrt{\frac{8K_d}{[M]_T[1 + ([S]/K_m)]} + \left(\frac{K_d}{[M]_T[1 + ([S]/K_m)]}\right)^2} \quad (17)$$

The value for λ is given by

$$\lambda = \frac{q}{(1 + K_m/[S])} \quad (18)$$

where k_{dis} is the dissociation rate constant for monomer/dimer exchange, k_{assoc} is the association rate constant for monomer–dimer exchange, q is given by

$$q = \{[k_{dis}(K_m/[S]) + 4k_{assoc}[M]_T(1 + K_m/[S])]^2 - [4k_{assoc}[M]_T(1 + K_m/[S])]^2\}^{1/2} \quad (19)$$

and finally the value for γ' is given by

$$\gamma' = \frac{4[M]_T(1 - \phi) + \frac{K_d}{(1 + [S]/K_m)} - \frac{q}{k_{assoc}(1 + K_m/[S])}}{4[M]_T(1 - \phi) + \frac{K_d}{(1 + [S]/K_m)} + \frac{q}{k_{assoc}(1 + K_m/[S])}} \quad (20)$$

RESULTS

Determination of Monomer–Dimer Rate Constants. A low-salt reaction, carried out in the absence of added inhibitor and initiated by the addition of concentrated HIV-1 protease stock, exhibits significant downward curvature (Figure 5A). The curvature is opposite when the enzyme is preincubated at low concentrations and the reaction is started by the addition of substrate. Both of these observations are consistent with reversible monomer–dimer exchange. Enzyme dilution, down to or below the K_d, results in dimer dissociation, whereas substrate addition to prediluted enzyme results in the net conversion of monomers into dimers due to the formation of a Michaelis complex. Integrated rate equations were developed for a simple two-state model (see Theory) and were applied to the data. Regressions for the monomer–dimer exchange required that one of the four parameters (k_{cat}, $[E]_T$, k_{assoc}, and k_{dis}) be fixed to known values: k_{cat} was fixed to 6.45 for high-salt conditions and $[M]_T$ was fixed to 2.69×10^{-10} M for low-salt conditions. Estimates for the kinetic rate constants were obtained from the regression analysis (Table 1).

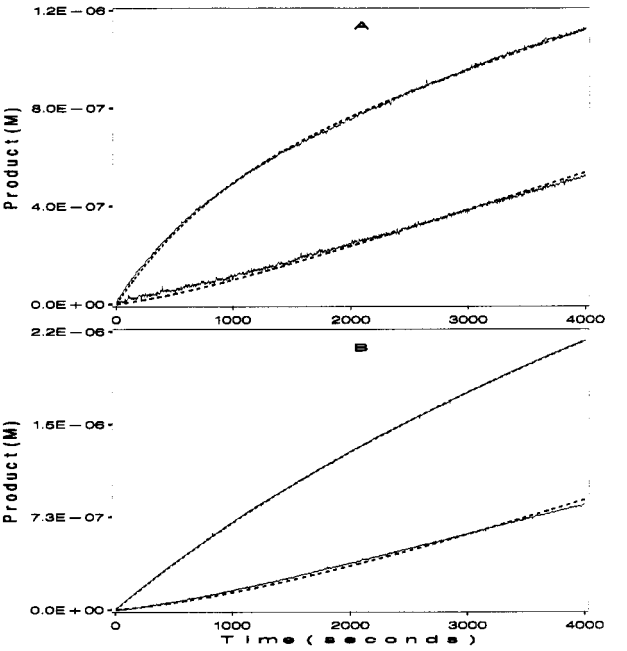

FIGURE 5: Paired progress curves for the monomer–dimer exchange. Raw fluorescence data (solid lines) were analyzed by a nonlinear regression fit (dashed lines) to the equations described in the Theory section for the association and dissociation of homodimeric enzyme. The parametric solutions for these analyses are shown in Table 1. The reaction is carried out under two different sets of assay conditions: (A) low-salt conditions with $K_m = 4.11 \times 10^{-6}$ M and (B) high-salt conditions where $K_m = 1.33 \times 10^{-6}$ M.

The amount of downward curvature shown for the enzyme inactivation process (Figure 5A) was unacceptable for the subsequent determination of inhibitor rate constants. Since it was not possible to derive equations for the simultaneous inactivation of HIV protease by these two competing events, it was necessary to reduce the contribution of the dimer dissociation process to the data. This was achieved by increasing the ES component of the reaction mixture and, hence, reducing the concentration of free homodimer. Substrate concentration could not be increased further since 1.0×10^{-5} M is at the limit of solubility, but the substrate binding affinity could be improved by increasing the salt concentration.

Consistent with a higher substrate binding affinity, data collected under high-salt conditions exhibit less downward curvature for the inactivation process (Figure 5B). The linear portion of this curve extends out to about 500 s, indicating that negligible enzyme inactivation has occurred. Consequently, a time course of 400 s and high-salt conditions were selected for the subsequent determination of inhibitor rate constants. The kinetic parameters obtained from the regression analysis are similar to those observed for low-salt conditions (Table 1). It should be noted that the substrate binding affinity constitutes the only significant difference between the two pairs of data sets.

Determination of Inhibitor Rate Constants. Paired progress curves were generated for BILA 398 using high-salt conditions (Figure 6). Parameter estimates from the nonlinear regression analysis are shown in Table 2. An identical analysis was

Table 1: Kinetic Rate Constants for Monomer–Dimer Interconversion[a]

expt	K_m ($\times 10^{-6}$ M)	$[M]_T$ ($\times 10^{-10}$ M)	k_{cat} (s^{-1})	k_{assoc} ($\times 10^5$ M^{-1} s^{-1})	k_{dis} ($\times 10^{-3}$ s^{-1})	K_d ($\times 10^{-9}$ M)
low salt	4.11 (±0.42)	2.69	7.35 (±0.02)	10.0 (±0.00)	2.59 (±0.01)	5.2
high salt	1.33 (±0.13)	2.69 (±0.00)	6.45	9.20 (±0.01)	1.86 (±0.01)	4.0

[a] Values for the fitted parameters were obtained from the nonlinear regression analysis to the raw data shown in Figure 5. The asymptotic standard errors of the regression are shown in parentheses.

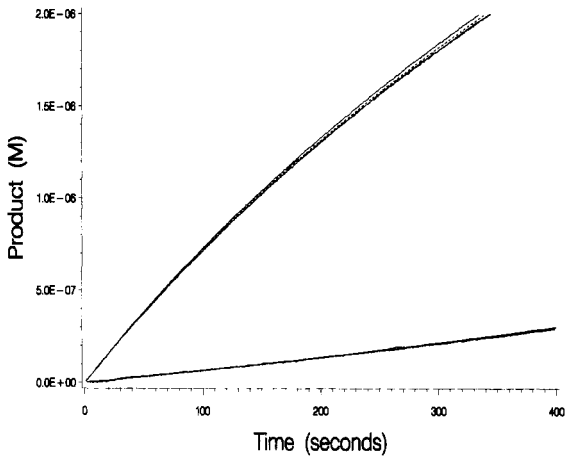

FIGURE 6: Paired progress curves for inhibitor binding. The inhibitor, BILA 398, was used to generate raw fluorescence data (solid lines) for the inhibition of HIV-1 protease. These data were analyzed by a nonlinear regression fit (dashed lines) to the equations described in the Theory section for the association and dissociation of competitive binding inhibitors. The parametric solutions for this analysis are shown in Table 2. The assay was conducted under high-salt conditions (K_m = 1.33 x 10^{-6} M) and with $[I]_T = 1.33 \times 10^{-9}$ M.

conducted on seven related inhibitors (data not shown). In these determinations, $[E]_T$ was increased by 2-fold. The values for k_{off} varied over 2 orders of magnitude, while little change was observed in the estimates for k_{cat}, $[E]_T$, and k_{on}. The average values for these invariant parameters, given with their standard deviations, were $k_{cat} = 6.45 \pm 1.27$, $[E]_T = (2.60 \pm 0.31) \times 10^{-9}$ M (this value is double that obtained above for BILA 398, as expected), and $k_{on} = (2.18 \pm 0.53) \times 10^{+7}$ M^{-1} s^{-1}. These values are similar to those obtained for BILA 398 (Table 2). In addition, the determination of $[E]_T$ also agrees very closely with the value of $[M]_T$ obtained from the monomer–dimer exchange experiment, given the additional 20-fold dilution factor (i.e., $20[M]_T/2 = 2.69 \times 10^{-9}$ M $\approx [E]_T$).

Steady State Determination of K_i. Inhibition data for BILA 398 were also analyzed by an independent and well-established method for the determination of K_i, as described. Similar K_i determinations were made on many other closely related inhibitors (data not shown). Discrepancies are often observed with estimated K_i both greater than and less than values determined by the paired progress curve method. Some possible explanations will be presented later (see Discussion).

DISCUSSION

The optimization of inhibitors as potential therapeutic agents usually is based on a comparison of K_i values. These determinations are easy to obtain and indicate the expected degree of enzyme inhibition at a given [I]. In contrast, the determination of rate constants for inhibition is a difficult process requiring nonequilibrium measurements and complex mathematical modeling. As a result, investigations of this type appear infrequently in the literature, even though they provide additional information about the inhibition system. In most cases, the most desirable inhibitor possesses a low k_{off}. The k_{on} is much less significant as the rate of inhibitor binding is seldom of therapeutic relevance. Calculations show that, for a target $[E]_T$ of 1×10^{-9} M, an *in vivo* $[I]_T$ of 1×10^{-7} M, and a k_{on} of 1×10^8 M^{-1} s^{-1}, equilibrium is reached within 1 s. Even for a slow-binding inhibitor with a k_{on} of 1×10^5 M^{-1} s^{-1}, equilibrium will be reached within the first several minutes. The k_{on} is relatively inconsequential since drug concentrations are usually maintained in plasma at many times the K_i for several hours. In contrast, the k_{off} is of significance since it indicates the lifetime of the inhibited complex and, hence, the duration of action. An inhibitor with a k_{on} of 1×10^8 M^{-1} s^{-1} and a k_{off} of 1×10^{-2} s^{-1} has the same K_i as a slow-binding inhibitor with a k_{on} of 1×10^5 M^{-1} s^{-1} and a k_{off} of 1×10^{-5} s^{-1}. These two inhibitors are indistinguishable on the basis of K_i, and yet the half-lives for dissociation vary from about 1 min to over 19 h!

Rate constants usually are determined in a multistep analytical process from either the onset of inhibition or the dissociation of an EI complex. In such cases, it frequently is not possible to achieve convergence to an unbiased solution. The reason for this is that while k_{on} and k_{off} both contribute to the observed rate for both reactions, k_{off} is most highly correlated with dissociation data and k_{on} with association data, resulting in a bias toward the less weighted rate constant. A further defect in the multistep analytical approach is that some parameters must be fixed so that subsequent regressions will successfully converge. The propagation of standard errors associated with fixed parameter values through to the final solution is complex. The paired progress curve method overcomes this drawback by the simultaneous solution of the four parameters, $[E]_T$, k_{cat}, k_{on}, and k_{off}. This is only possible because of the pairing of both association and dissociation data in the same analysis.

In this report, the paired progress curve method has been applied to two different enzyme inactivation processes: (1) competitive inhibition by a substrate analog and (2) dimer dissociation to inactive monomers. A complete understanding of both processes is essential for the selection of a potential AIDS therapeutic. The dissociation of HIV protease obscures the contribution of inactivation by an active site inhibitor, making an accurate determination of rate constants difficult. Furthermore, monomer–dimer interconversion is of physiological relevance as it has been shown to be critical in the viral maturation process (Kräusslich, 1991).

Rate constants for the monomer–dimer interconversion were found to be very similar for both low- and high-salt assay conditions. The different curve shapes observed result from the two distinct values of K_m. This is in contrast to published work showing a 15-fold increase in K_d resulting from a 1 M decrease in salt concentration (Kuzmic et al., 1993). Results shown here also indicate that the rate of dimer dissociation takes place slowly. The half-life for dissociation is 350 s, given a k_{dis} of 2.0×10^{-3} s^{-1}. The inactivation rate is reduced further since only free enzyme is able to dissociate (Kuzmic et al., 1993). For example, approximately 7% of the enzyme used in the inhibition experiment will have dissociated by 400 s, given a starting concentration of homodimer of 3.0×10^{-10} M (see eq 3). The rate of monomer association is also slow: a k_{assoc} of 9×10^5 M^{-1} s^{-1} lies well below the diffusion control limit for small molecules. Possibly this is due to the

Table 2: Kinetic Rate Constants for Inhibitor Binding[a]

expt	$[E]_T$ ($\times 10^{-9}$ M)	k_{cat} (s^{-1})	k_{on} ($\times 10^{+7}$ M^{-1} s^{-1})	k_{off} ($\times 10^{-4}$ s^{-1})	K_i ($\times 10^{-12}$ M)
I	1.35 (±0.02)	6.68 (±0.08)	1.53 (±0.02)	1.03 (±0.13)	6.7
II	1.36 (±0.02)	7.49 (±0.09)	1.77 (±0.02)	0.61 (±0.14)	3.5
III	1.24 (±0.02)	7.32 (±0.09)	1.54 (±0.01)	1.37 (±0.09)	8.9

[a] Values for the four parameters were obtained from the nonlinear regression analysis in three separate experiments. The asymptotic standard errors of the regression are shown in parentheses.

requirement for monomer refolding and dimerization in a single step.

There are many published values for kinetic and equilibrium constants involved in the dimerization process: (1) $K_d = 3.6 \times 10^{-9}$ M was determined (Zhang et al., 1991); (2) k_{assoc} and k_{dis} were determined (Cheng et al., 1990) to be 7.0×10^4 M^{-1} s^{-1} and 3.5×10^{-3} s^{-1}, respectively, resulting in a K_d of 50×10^{-9} M; (3) a K_d of 39×10^{-12} M was obtained by monitoring urea-mediated protein unfolding (Grant et al., 1992); and (4) low K_d values (picomolar range) were estimated by analyzing variations in specific activity as a function of varying $[E]_T$ (Jordan et al., 1992). Most of the variance is probably due to different assay conditions. In one case (Jordan et al., 1992), the authors assume a rapid dissociation process. Data obtained in this report indicate that this assumption is invalid.

Several different methods of analysis were used for the determination of K_i values for many different compounds related to BILA 398. Initial determinations relied heavily on steady state methods, such as those described herein, and on the method of active site titration (substitution of v_z for v_s in eq 6). The method of active site titration was found to be inaccurate as significant dimer dissociation occurred during the preincubation of enzyme with low $[I]_T$. The steady state method was found to give reliable values for K_i, but estimates for $[E]_T$ were found to be highly variable, contain large asymptotic standard errors, and occasionally give $[E]_T$ values less than zero. As it was not possible to predict the impact of an inaccurate $[E]_T$ on the estimate for K_i, a method was desired that could determine both constants with acceptable statistics. This search culminated in the development of the paired progress curve method.

K_i values determined by the paired progress curve method and the steady state method were found to differ, often substantially, for a series of related inhibitors. Defects in the steady state method involve various uncertainties: (1) the determination of v_s is an extrapolation from a pre-steady state condition; (2) v_s is determined from an equation describing non-tight-binding inhibition, i.e., the concentration of free [I] is incorrectly assumed to be equal to $[I]_T$; and (3) the steady state methods involve titrations with $[I]_T$ less than $[E]_T$, conditions under which dimer dissociation is accelerated. Defects in the paired progress curve method involve the following: (1) small values of k_{off} are estimated by the paired progress curve method on the basis of very small amounts of EI dissociation and, hence, entail large extrapolations, and (2) EI dissociation data for the paired progress curve method require that enzyme and inhibitor be preincubated for a period of time during which dimer dissociation will occur. Further work is in progress to resolve these discrepancies.

There are several advantages of the paired progress curve method over those methods currently in use: (1) the method is rapid; (2) data collection is experimentally simple as it is conducted at a single [S], a single $[E]_T$, and a single $[I]_T$; (3) the nonlinear regression analysis usually converges to a solution; (4) estimates for $[E]_T$, k_{cat}, k_{on}, and k_{off} are determined simultaneously; and (5) these values are presented with acceptable statistics. These advantages make the paired progress curve method of analysis unique within those methods currently available.

ACKNOWLEDGMENT

We thank Chris Grygon for helpful discussions and guidance on the use of fluorescence spectroscopy. To John J. Miglietta and Anthony Shrutkowski we are grateful for the PCR work on HIV-1 protease, and we also thank Diane Thibeault, Christian Yoakim, and Peter Grob for their insight and support throughout this project.

REFERENCES

Babé, L. M., Rosé, J., & Craik, C. S. (1992) *Protein Sci. 1*, 1244–1253.

Bevington, P. R. (1969) in *Data Reduction and Error Analysis for the Physical Sciences,* pp 56–65, McGraw-Hill Book Company, New York.

Cha, S. (1980) *Biochem. Pharmacol. 29*, 1779–1789.

Cheng, Y. E., Yin, F. H., Foundling, S., Blomstrom, D., & Kettner, C. A. (1990) *Proc. Natl. Acad. Sci. U.S.A. 87*, 9660–9664.

Debouck, C., & Metcalf, B. W. (1990) *Drug Dev. Res. 21*, 1–17.

Frieden, C., Kurz, L. C., & Gilbert, H. R. (1980) *Biochemistry 19*, 5303–5309.

Grant, S. K., Deckman, I. C., Culp, J. S., Minnich, M. D., Brooks, I. S., Hensley, P., DeBouck, & C., Meek, T. D. (1992) *Biochemistry 31*, 9491–9501.

Greco, W. R., & Hakala, M. T. (1979) *J. Biol. Chem. 254*, 12104–12109.

Hahn, B. H., Shaw, G. M., Arya, S. K., Popovic, M., Gallo, R. C., & Wong-Staal, F. (1984) *Nature 312*, 166–169.

Jordan, S. P., Zugay, J., Darke, P. L., & Kuo, L. C. (1992) *J. Biol. Chem. 267*, 20028–20032.

Kaplan, A. H., Zack, J. A., Knigge, M., Paul, D. A., Kempf, D. J., Norbeck, D. W., & Swanstrom, R. (1993) *J. Virol. 67*, 4050–4055.

Kräusslich, H. (1991) *Proc. Natl. Acad. Sci. U.S.A. 88*, 3213–3217.

Matayoshi, E. D., Wang, G. T., Krafft, G. A., & Erickson, J. (1990) *Science 247*, 954–958.

Morrison, J. F., & Stone, S. R. (1985) *Comm. Mol. Cell. Biophys. 2*, 347–368.

Sculley, M. J., & Morrison, J. F. (1986) *Biochim. Biophys. Acta 874*, 44–53.

Studier, F. W., & Moffat, B. A. (1986) *J. Mol. Biol. 189*, 113–130.

Studier, F. W., Rosenberg, A. H., Dunn, J. J., & Dubendorff, J. W. (1990) *Methods Enzymol. 185*, 60–89.

Tong, L., Pav, S., Pargellis, C., Do, F., Lamarre, D., & Anderson, P. C. (1993) *Proc. Natl. Acad. Sci. U.S.A. 90*, 8387–8391.

Williams, J. W., & Morrison, J. F. (1979) *Methods Enzymol. 63*, 437–467.

Williams, J. W., Morrison, J. F., & Duggleby, R. G. (1979) *Biochemistry 18*, 2567–2573.

Zhang, Z., Poorman, R. A., Maggiora, L. L., Heinrikson, R. L., & Kézdy, F. J. (1991) *J. Biol. Chem. 266*, 15591–15594.

Zimmerle, C. T., & Frieden, C. (1989) *Biochem. J. 258*, 381–387.